Convergence: Journal of Multidisciplinary Research and Innovation
https://www.iahiservices.com

Original Research Article

Moisture-Dependent Granular Flow, Stratification, and Stone–Grain Segregation Dynamics in Vibratory Gravity Rice De-Stoning Systems

Article Section: Physical Sciences and Engineering

N.A Mbakaan[1] https://orcid.org/0009-0009-0108-0544 S.E Obetta[2] O.J Ijabo[3]

[1, 2, 3]Department of Agricultural and Biosystems Engineering, Joseph Sarwuan Tarka University, P.M.B. 2373, Makurdi, Benue State, Nigeria.

Corresponding Author E-mail: nathanieaondoyila@gmail.com Tel: +2349030958907

Abstract- Moisture-dependent granular segregation remains a critical limitation in vibratory gravity rice de-stoning systems, where stones and grains exhibit overlapping size distributions but differ in density, morphology, and surface properties. Although granular segregation under gravity and vibration has been widely studied, most existing investigations focus on dry or idealized particle systems, providing limited insight into realistic agricultural materials where moisture-induced cohesion plays a dominant role. Unlike previous studies focused on dry or idealized particles, this work provides experimentally validated evidence of nonlinear moisture–vibration–gravity coupling in realistic agricultural granular systems. This study experimentally investigates the coupled effects of moisture content, vibration kinematics, and gravity on granular flow, stratification, and stone–grain segregation in a vibratory gravity rice de-stoner using FARO-44 and NERICA-11 rice varieties. Experiments were conducted at moisture contents of 10–14% (wet basis), shaker angles of 12–15°, and varying pulley diameters using a factorial experimental design combined with analysis of variance and response surface methodology. Results show that stone recovery efficiency decreases monotonically with increasing moisture content due to capillary-induced cohesion, which suppresses kinetic sieving and density-driven percolation. Shaker angle emerged as the dominant mechanical control parameter, with 15° providing optimal stratification through a balance of gravitational transport and vibration-induced lift, while pulley diameter contributed primarily through interaction effects by stabilizing vibratory energy transmission. Quadratic response surface models exhibited strong predictive capability ($R^2 > 0.90$), confirming the nonlinear nature of moisture–vibration–gravity interactions. Multi-objective optimization identified an optimal operating condition of 144 mm pulley diameter, 15° shaker angle, and 10% moisture content for FARO-44 rice, achieving approximately 84% cleaning efficiency, 57 kg h^{-1} throughput, and 690 kg per 12 h capacity with a desirability index of 0.991. The findings provide a physics-based interpretation of moisture-controlled granular segregation and offer a statistically validated operational framework for improving separation efficiency in vibratory gravity de-stoning systems.

Article Key Information

Keywords: Moist granular flow; Vibratory gravity separation; Stone–grain segregation; Granular stratification

Received: 20th November 2025 **Revised:** 5th January, 2026 **Accepted**: 20th January, 2026 **Published**: 24th January 2026

1.0 Introduction

Granular materials are ubiquitous in both natural and engineered systems, spanning applications from geophysical mass movements to agricultural and industrial particle processing. Unlike classical solids or fluids, granular media exhibit highly nonlinear and non-equilibrium behavior governed by particle-scale interactions, external forcing, and environmental conditions. Under gravity and vibration, granular assemblies display complex phenomena such as stratification, convection, percolation, and segregation, which strongly influence flow efficiency and separation performance in vibratory systems [1], [2].

A persistent challenge in granular processing is stone–grain segregation, particularly in agricultural products such as rice, where stones and grains often share overlapping size distributions but differ in density, shape, and surface properties. Gravity-based vibratory separators exploit these physical contrasts by combining inclined oscillating decks with vibration and, in some cases, airflow to induce stratification and directional transport [3]. However, separation efficiency in such systems is highly sensitive to operating conditions, especially moisture content, which modifies inter-particle forces, contact mechanics, and flow regimes.

Segregation in dry granular flows is commonly explained by mechanisms such as kinetic sieving and squeeze expulsion, whereby smaller or denser particles preferentially percolate downward through voids created during shear, while larger or lighter particles migrate upward [4]. In vibratory gravity systems, these mechanisms coexist with vibration-induced convection and frictional anisotropy, leading to layered structures or longitudinal stratification along the deck surface [5]. Previous studies have demonstrated that vibration frequency, amplitude, and deck inclination govern particle mobility and residence time, thereby exerting a strong influence on separation efficiency [6], [7].

The introduction of moisture fundamentally alters granular behavior. Even small amounts of water generate liquid bridges between particles, producing capillary cohesion that increases resistance to motion and modifies contact mechanics [8]. As a result, moist granular materials typically exhibit higher angles of repose, reduced flowability, and altered stress transmission compared to dry systems [9]. In vibratory separators, moisture can suppress kinetic sieving by limiting particle rearrangement, while simultaneously enhancing adhesion between grains and stones, leading to reduced stratification clarity.

Experimental and theoretical studies have shown that moisture content governs transitions between granular flow regimes. At low moisture levels, capillary forces dominate, producing cohesive clusters that resist segregation; at higher moisture contents, lubrication effects and pore pressure buildup can partially fluidize the granular bed, restoring particle mobility [10], [11]. This non-monotonic response makes moisture a critical but challenging parameter to control in practical separation systems, particularly in tropical agricultural contexts where ambient humidity and post-harvest handling conditions vary widely.

Vibration further complicates moisture-dependent granular dynamics. Vibratory excitation can intermittently break liquid bridges and reduce effective friction, depending on acceleration levels and contact durations [12]. Investigations of vibrated wet granular beds have revealed that segregation trends observed under dry vibration may weaken, reverse, or vanish entirely under moist conditions [13]. These observations indicate that classical dry-granular segregation theories are insufficient when moisture and vibration act simultaneously.

Recent advances in discrete element method (DEM) simulations and high-speed experimental diagnostics have enabled deeper insight into particle-scale dynamics in moist granular systems [14], [15]. These tools reveal that segregation outcomes depend on coupled effects of particle density contrast, moisture-induced cohesion, vibration intensity, and gravitational forcing. However, most existing studies focus on idealized spherical particles or dry conditions, limiting direct applicability to agricultural grains, which are irregular, anisotropic, and exhibit variable surface roughness.

Within this context, the present paper constitutes a focused extraction from a broader experimental investigation of a vibratory gravity rice de-stoning system, which examined machine performance, operational optimization, and separation efficiency under varying moisture conditions. Rather than addressing the full engineering design and optimization scope of the parent study, this paper concentrates specifically on the moisture-dependent granular flow behavior, stratification mechanisms, and stone–grain segregation dynamics that govern separation outcomes in such systems.

Accordingly, the objective of this study is to elucidate the coupled roles of moisture content, vibratory excitation, and gravitational forcing in governing granular flow behavior, stratification, and segregation efficiency in stone–grain mixtures representative of rice de-stoning operations. By systematically integrating controlled experimental observations with established theories of granular flow and segregation, this work seeks to bridge the gap between idealized dry-granular models and the complex, moisture-affected conditions encountered in practical agricultural processing systems. In doing so, the study advances the fundamental understanding of moist granular dynamics in vibrated inclined beds while providing a physically grounded interpretation of separation behavior in vibratory gravity de-stoning equipment. Specifically, the contributions of this work include: (i) quantitative characterization of moisture-induced suppression of kinetic sieving and density-driven percolation under vibratory excitation, (ii) identification of shaker angle as the dominant mechanical parameter regulating stratification intensity and segregation efficiency in moist granular beds, and (iii) establishment of statistically validated operating regimes that link granular physics with practical performance optimization in vibratory gravity de-stoning systems.

2.0 Literature Review

2.1 Granular Flow and Segregation under Gravity

Early foundational studies established that granular materials subjected to gravity-driven shear exhibit segregation rather than homogeneous mixing. Jaeger et al. [1] and the GDR MiDi consortium [2] demonstrated that dense granular flows possess rheological properties distinct from classical fluids, with stress transmission governed by enduring contacts and force chains. Within this framework, kinetic sieving was identified as a dominant segregation mechanism, particularly in gravity-driven surface flows, where smaller particles preferentially percolate downward through transient voids generated during shear [16].

Gray and Thornton [17] formalized this process using continuum segregation models, showing that size and density contrasts lead to stratified flow structures in inclined granular layers. Their work demonstrated that segregation flux scales with shear rate and local concentration gradients, providing a predictive basis for stratification formation. Subsequent experimental investigations confirmed that gravity-driven segregation results in layered deposits, with coarse or dense particles accumulating at the base and finer particles migrating upward [18]. These mechanisms are directly relevant to vibratory gravity separators, where inclined decks exploit similar gravity-assisted percolation processes to initiate stone–grain separation.

However, gravity-driven segregation alone cannot fully account for the dynamics observed in mechanically agitated systems. In practical de-stoning machines, gravity-induced percolation interacts strongly with vibration-induced particle rearrangement, necessitating a broader theoretical framework that incorporates external excitation effects.

2.2 Vibration-Induced Granular Stratification and Convection

Vibration fundamentally alters granular flow behavior by intermittently reducing interparticle friction and contact persistence. Classical investigations of vertically vibrated granular beds revealed the emergence of convection cells, vibrofluidization, and density-driven segregation phenomena commonly referred to as the Brazil nut effect [7], [12]. Knight et al. [19] experimentally demonstrated that vibration generates convection rolls, which transport larger particles upward while smaller particles migrate downward near the container boundaries.

Further studies established that vibration frequency and acceleration amplitude govern transitions between quasi-static, convective, and fully fluidized regimes [20]. Tripathi and Khakhar [5] showed that in vibrofluidized beds, density differences alone can drive segregation even when particle sizes are similar, a condition frequently encountered in stone–grain mixtures used in agricultural processing. These findings are particularly significant for rice de-stoning systems, where stones and grains often overlap in size but differ in density and surface roughness.

Importantly, stratification in vibratory systems is not limited to vertical segregation. Chandratilleke et al. [6] observed longitudinal stratification along inclined vibratory decks, where particles segregate spatially according to differential transport velocities. Such directional transport mechanisms are absent in purely gravity-driven flows but are central to the operation of vibratory gravity separators.

2.3 Moisture Effects in Granular Materials

The presence of moisture introduces additional complexity into granular systems through capillary cohesion and lubrication effects. Herminghaus [8] and Mitarai and Nori [9] provided comprehensive reviews of wet granular physics, demonstrating that even small liquid contents generate capillary bridges that significantly modify interparticle forces. These cohesive forces increase yield stress, suppress relative particle motion, and alter flow regimes compared to dry granular systems.

Experimental studies of wet granular flows have shown that moisture induces non-monotonic mechanical behavior. Fall et al. [11] reported that low moisture contents increase resistance to shear due to capillary cohesion, whereas higher moisture levels can reduce effective friction through lubrication and pore pressure effects. In gravity-driven collapses and avalanches, moisture has been shown to reduce flow mobility at low saturation but enhance runout at higher saturation due to partial fluidization [10], [21]. These observations indicate that moisture modifies not only bulk flow behavior but also internal particle rearrangement pathways relevant to segregation processes.

In agricultural materials, such moisture-dependent changes in flowability and cohesion directly affect separation efficiency, making moisture content a critical operational parameter in practical de-stoning systems.

2.4 Moisture-Dependent Segregation and Vibration Coupling

Only a limited number of studies have examined the combined effects of moisture and vibration on granular segregation. Wassgren et al. [13] investigated cohesive granular flow in vibrated beds and found that increasing cohesion suppresses size segregation by inhibiting kinetic sieving, indicating that classical dry-granular segregation models are inadequate under moist conditions. Eshuis et al. [12] demonstrated that vibratory excitation can intermittently rupture liquid bridges depending on acceleration levels, suggesting that vibration may partially counteract moisture-induced cohesion.

Discrete element method (DEM) studies incorporating capillary force models have further confirmed that segregation efficiency decreases sharply with increasing cohesion unless vibration intensity is sufficiently high to overcome adhesive forces [14], [22]. Despite these advances, most investigations focus on idealized spherical particles and assume uniform wetting, which limits their applicability to agricultural grains that are irregular, anisotropic, and exhibit variable surface roughness and localized moisture heterogeneities.

2.5 Research Gaps and Motivation

The reviewed literature reveals several critical gaps relevant to vibratory gravity rice de-stoning systems. First, systematic studies addressing stone–grain segregation under the combined influence of gravity, vibration, and moisture remain scarce. Second, existing segregation theories are predominantly developed for dry or idealized systems and do not adequately capture cohesion-driven transitions observed in moist granular flows. Third, the interaction between vibration parameters and moisture-induced forces remains poorly quantified for practical separator geometries and realistic agricultural particle shapes.

Given the economic and food-security implications of efficient rice de-stoning, particularly in developing regions, there is a clear need for experimentally grounded, physics-based understanding of moisture-dependent granular segregation. The present study builds upon established granular flow and segregation literature by explicitly focusing on moisture-dependent stratification and stone–grain segregation dynamics in vibratory gravity systems, thereby extending both theoretical understanding and practical applicability.

3.0 Materials and Methods

3.1 Materials

Two commercially milled rice varieties, Sipi (FARO-44) and Mass (NERICA-11), were obtained from a rice mill in Wurukum, Makurdi, Benue State, Nigeria. These varieties were selected because of their contrasting grain morphology and density, which are known to influence moisture-dependent stratification and segregation in vibratory gravity separation systems.

All measuring instruments were calibrated before experimentation. The instruments included a digital vernier caliper (±0.01 mm), electronic balance (±0.01 g), measuring cylinder, bottomless cylindrical container, moisture meter (6–40%), air-velocity tunnel with anemometer, and test surfaces of galvanized steel, plastic, and glass.

3.2 Physical Property Determination

The physical properties of rice grains were determined following the standardized procedure of Kayodele *et al.* [23]. These properties were measured to provide a mechanistic explanation for stratification and segregation trends observed in the vibratory system.

The measured properties included bulk density (ρ_b), true density (ρ_s), porosity (ε), thousand-grain mass (M_{1000}), specific gravity (SG), axial dimensions (L, W, T), geometric mean diameter (D_g), angle of repose (θ_r), and angles of friction on different structural surfaces.

Bulk density was determined as:

$$\rho_b = \frac{M}{V}$$

where M is the mass of rice (kg) and V is the container volume (m³).

True density was obtained using liquid displacement:

$$\rho_s = \frac{M}{V_s}$$

Porosity was computed as:

$$\varepsilon = \left(1 - \frac{\rho_b}{\rho_s}\right) \times 100$$

Specific gravity was evaluated as:

$$SG = \frac{\rho_s}{\rho_w}$$

where ρ_w is the water density at laboratory temperature.

The geometric mean diameter was calculated as:

$$D_g = (LWT)^{1/3}$$

The angle of repose was obtained using:

$$\tan\,\theta_r = \frac{h}{r}$$

Angles of friction were determined on galvanized steel, plastic, and glass surfaces by gradual inclination until sliding commenced.

3.3 Moisture Content Conditioning

Moisture content on a wet basis was determined as:

$$MC_{wb} = \frac{M_w}{M_t} \times 100$$

where M_w is the mass of water and M_t is the total wet mass.

Samples were conditioned to 10, 12, and 14% moisture by adding calculated distilled water, sealing in polyethylene bags, and equilibrating for 24 h. Moisture variation was introduced to evaluate its influence on granular cohesion, stratification, and segregation efficiency.

3.4 Aerodynamic Characterization

The terminal velocity of rice grains and stones was measured using an air-velocity tunnel. Terminal velocity corresponds to the condition where gravitational force equals drag force. Reynolds number was calculated as:

$$Re = \frac{\rho V_t D}{\mu}$$

These parameters were used to explain differences in particle suspension and stratification behavior in the vibratory gravity field.

3.5 Design and Vibratory–Aerodynamic Separation Mechanism of the Rice De-stoning System

Figure 1 illustrates the detailed engineering representations of the fabricated rice de-stoning machine, including orthographic, exploded, and isometric views. The machine consists of a rigid steel frame supporting a vibratory inclined sieve deck, feed hopper, axial airflow unit, belt–pulley transmission system, eccentric vibration mechanism, and separate discharge outlets for rice and stone fractions.

The sieve deck is mounted on elastic supports and driven by an eccentric shaft connected to the pulley system, which converts rotary motion from the electric motor into controlled reciprocating vibration. The inclination of the deck is adjustable, allowing regulation of particle residence time and transport velocity along the sieve surface. The perforated deck permits upward airflow supplied by the axial fan positioned beneath the sieve.

The separation process is based on the combined effects of vibration, gravity, and aerodynamic lift. When the rice–stone mixture is introduced through the hopper onto the vibrating deck, vibration induces stratification within the granular bed. Denser and heavier stone particles migrate downward toward the sieve surface, while lighter rice grains remain in the upper layer. This stratification behavior is consistent with the aerodynamic property differences established in Section 3.4.

The inclined deck simultaneously promotes differential lateral transport. Stone particles, having higher contact friction and lower susceptibility to aerodynamic lift, move predominantly along the deck surface toward the stone discharge outlet. In contrast, rice grains experience greater vibratory mobility and partial aerodynamic support, causing them to migrate toward the rice outlet.

Upward airflow through the sieve further enhances separation by partially fluidizing the granular bed, reducing inter-particle friction and improving particle mobility. Because stone particles possess higher terminal velocities than rice grains, they are less affected by the airflow and remain in contact with the sieve, while rice grains are preferentially transported by the combined vibratory and aerodynamic actions.

The operational behavior of the system is governed by adjustable parameters including deck inclination angle (α), vibration frequency (f), vibration amplitude (A), air velocity (V_a), feed rate (Q), and pulley diameter (D_p). These parameters jointly control bed thickness, residence time, stratification intensity, and particle trajectory, thereby determining the overall de-stoning efficiency.

Figure 1, therefore, provides a comprehensive visualization of the machine structure, component integration, and mechanical layout, forming the basis for understanding the experimental performance and optimization results discussed in subsequent sections.

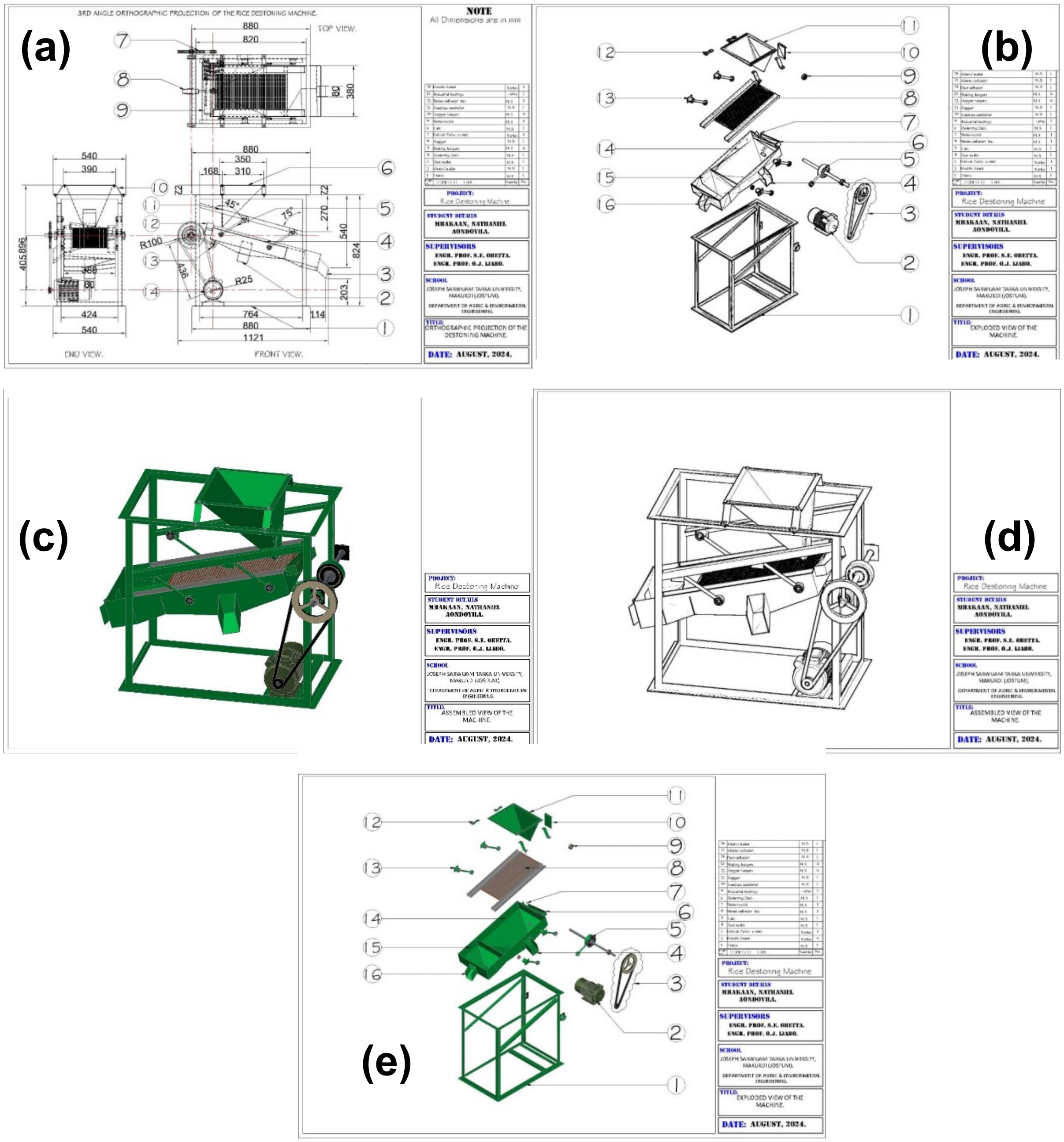

Figure 1. Engineering representations of the rice de-stoning machine: (a) orthographic projection showing front, top, and side views with key dimensional references; (b) exploded view illustrating component arrangement and assembly sequence; (c) isometric view of the fully assembled machine; (d) alternative isometric perspective highlighting the

hopper, vibrating deck, and discharge outlets; and (e) detailed exploded view emphasizing internal mechanical and transmission components.

3.6 Development and Fabrication of the Rice De-stoning Prototype

The rice de-stoning prototype used in this study was developed as the physical realization of the separation concept described in Section 3.5 and fabricated to ensure mechanical stability, repeatability, and controlled adjustment of operating parameters during experimentation. Emphasis was placed on structural rigidity, vibration transmission efficiency, and ease of parameter variation rather than optimization for industrial mass production.

The supporting frame was fabricated from mild steel angle bars selected for their availability, weldability, and ability to withstand cyclic vibratory loading without excessive deformation. All structural joints were permanently welded to minimize energy dissipation and to maintain alignment of the vibrating components during operation. The overall frame configuration of the fabricated machine is shown in Figure 2(a–c).

The vibratory sieve deck was constructed from perforated galvanized steel sheet to provide adequate strength, corrosion resistance, and uniform airflow distribution. The deck was mounted on elastic supports that allowed controlled reciprocating motion while preventing rigid-body resonance. Adjustable mounting slots and fasteners were incorporated to permit systematic variation of the deck inclination angle over the experimental range without compromising structural integrity.

Vibratory excitation was generated using an eccentric shaft assembly coupled to an electric motor through a belt–pulley transmission system. Interchangeable pulleys were employed to vary vibration frequency and amplitude indirectly while maintaining constant motor speed. The physical implementation of the shaker mechanism and its mounting arrangement are clearly illustrated in the end view of the prototype shown in Figure 2(c).

An axial airflow unit was installed beneath the sieve deck to supply upward airflow through the perforations. The airflow system was mechanically isolated from the vibrating frame to prevent vibration-induced fluctuations in air velocity and to ensure stable aerodynamic conditions during experimentation.

Separate discharge outlets were fabricated for rice grains and stone impurities to allow clear separation, collection, and mass measurement after each experimental run. The outlet geometry was designed to prevent material re-entry or cross-contamination between fractions during operation.

Overall, the fabricated prototype (Figure 2) was designed to provide dimensional stability, mechanical repeatability, and operational flexibility. These characteristics ensured that observed separation behavior and performance trends resulted from controlled variations in moisture content, vibration parameters, and deck inclination angle rather than from uncontrolled structural or mechanical effects.

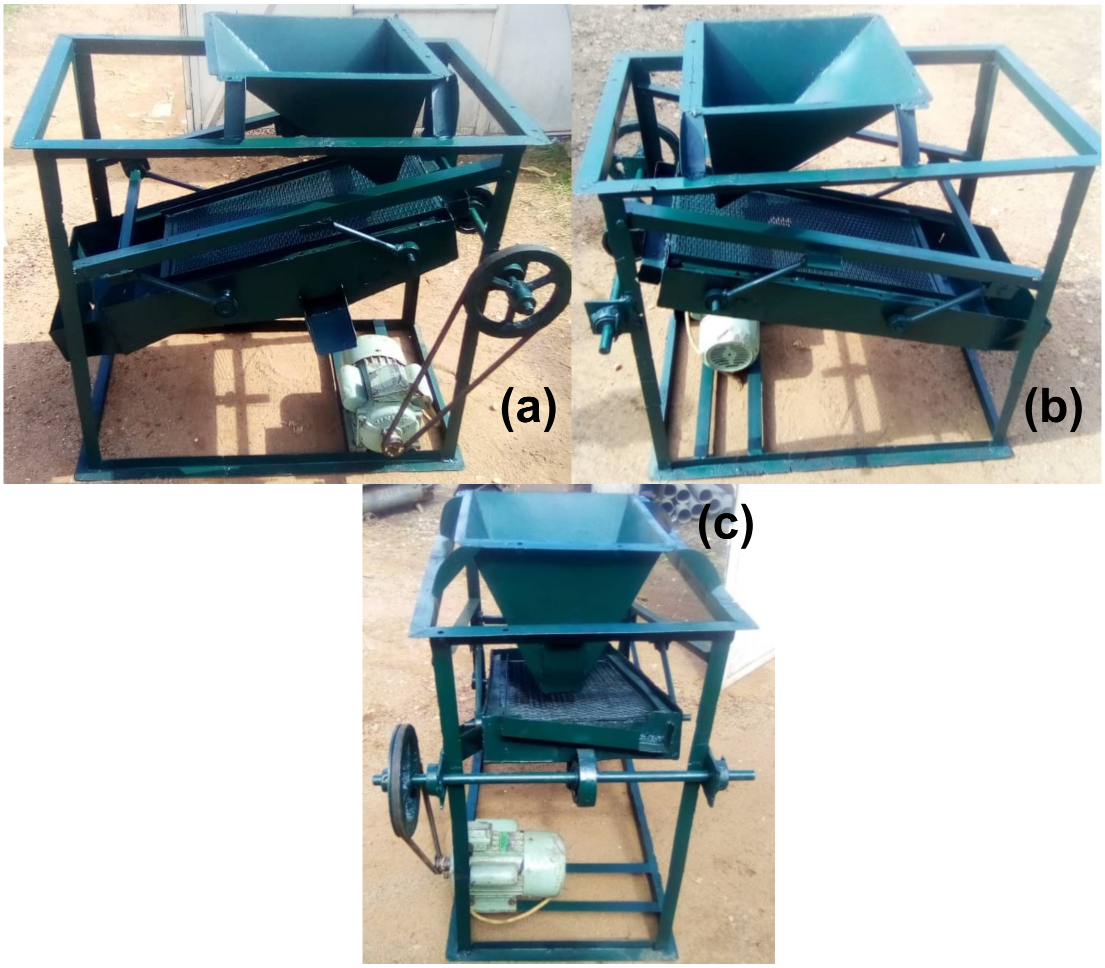

Figure 2 (a) Side View of Developed Rice De-stoning Machine (b) Another Side View of Developed Rice De-stoning Machine (c) End view of the rice-destoner showing the Shaker Mechanism

3.7 Experimental Design

A factorial experimental design was used to evaluate the combined effects of moisture content, shaker angle, pulley diameter, and rice variety on segregation behavior. Each run was replicated three times.

3.8 Data Integrity Control

Triplicate measurements were averaged. Instruments were periodically recalibrated. Environmental conditions were monitored to minimize systematic error.

4.0 Results and Discussion

The performance of the developed prototype described in Section 3 was evaluated under different operating conditions, and the corresponding experimental results are presented and discussed in the following subsections.

4.1 General Performance Trends of the Vibratory De-Stoning System

The experimental performance of the vibratory gravity rice de-stoning system under varying moisture contents (10–14% wb), shaker angles (12°–15°), pulley diameters, and rice varieties is summarized in Tables 1(a–b). Statistical significance of the process variables and their interactions is presented in Tables 2 and 3, while the interaction and optimization trends are illustrated in Figures 3–5.

Across all operating conditions, the system exhibited strong sensitivity to moisture content and shaker angle, confirming that granular segregation in vibratory gravity separators is primarily governed by moisture-dependent inter-particle cohesion and vibration-induced stratification mechanisms, as reported in vibrated granular bed studies by Zhang et al. [24] and Remy et al. [25].

4.2 Moisture-Dependent Stone Recovery Efficiency

As shown in Table 1(a), stone recovery efficiency decreased consistently as moisture content increased from 10% to 14% for both FARO-44 and NERICA-11 rice varieties. At 10% moisture, FARO-44 recorded the highest recovery values, while performance declined progressively at 12% and 14% moisture levels.

Table 1. Mean Stone Recovery Results of the Prototype De-Stoner under Different Moisture Contents, Varieties, Pulley Diameters, and Shaker Angles

(a) Effect of Pulley Diameter on Stone Recovery (Mean of Three Replicates)

Moisture Content (% wb)	Variety	Pulley 1	Pulley 2	Pulley 3
10%	FARO-44	218.77	228.48	237.44
10%	NERICA-11	221.39	210.56	232.59
12%	FARO-44	195.33	204.00	212.00
12%	NERICA-11	197.67	188.00	207.67
14%	FARO-44	191.43	199.92	207.76
14%	NERICA-11	191.43	199.92	207.76

(b) Effect of Shaker Angle on Stone Recovery (Mean of Three Replicates)

Moisture Content (% wb)	Variety	12°	14°	15°
10%	FARO-44	258.72	254.24	269.92
10%	NERICA-11	228.48	241.92	253.12
12%	FARO-44	231.00	227.00	241.00
12%	NERICA-11	204.00	216.00	226.00
14%	FARO-44	226.38	222.46	236.18
14%	NERICA-11	199.92	211.68	221.48

This behavior is attributed to the formation of liquid bridges between particles at elevated moisture levels, which increases cohesive forces and suppresses particle mobility. The resulting reduction in kinetic sieving and density-driven percolation limits the downward migration of stones through the rice bed. Similar moisture-induced suppression of segregation has been experimentally demonstrated in vibrated granular systems by Zhang et al. [24] and Remy et al. [25].

These findings confirm that optimal segregation occurs under near-dry conditions where frictional and collisional interactions dominate over cohesive bonding.

4.3 Effect of Shaker Angle on Stratification Dynamics

The influence of shaker angle on segregation efficiency is clearly demonstrated in Table 1(b) and the interaction plots in Figures 3(a) and (b). Stone recovery increased as shaker angle increased from 12° to 15° across all moisture levels and for both rice varieties.

At 15°, the system consistently achieved the highest segregation efficiency. This improvement results from the combined effect of increased downslope gravitational force and sustained vibratory lift, which enhances vertical stratification of the particle bed. Under such conditions, denser stone particles migrate downward while lighter rice grains are transported upward, consistent with the Brazil-nut and reverse Brazil-nut segregation mechanisms described by Rosato et al. [26] and Gray and Thornton [27].

The statistically significant moisture–shaker interaction observed in Figures 3(a) and (b) further confirms that the effectiveness of the shaker angle is strongly moisture-dependent.

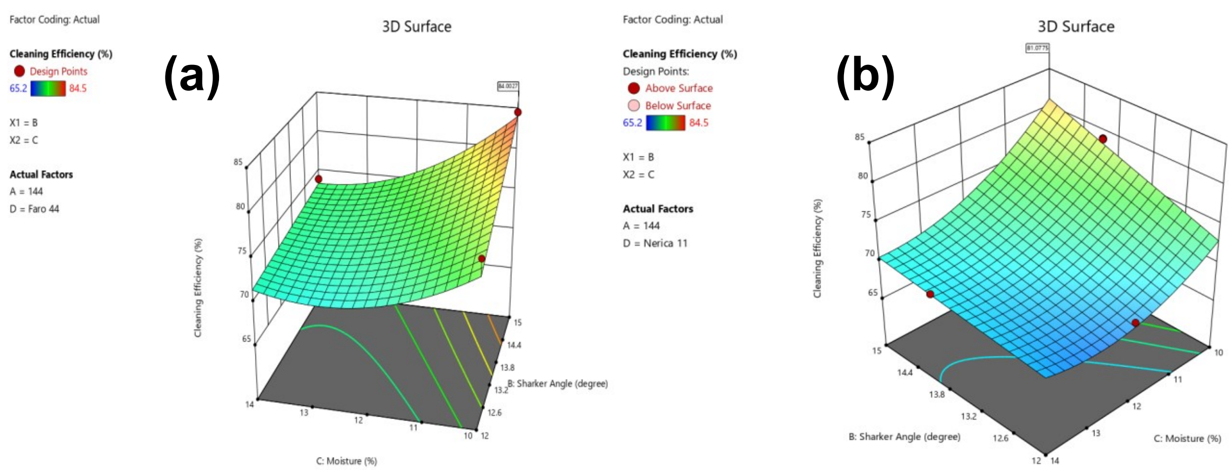

Figure 3: Effect of interaction of moisture and shaker angle being significant to de-stoning efficiency according to ANOVA for (a) Faro 44 and (b) Nerica-11

4.4 Influence of Pulley Diameter on Vibratory Transport

Pulley diameter exhibited a comparatively weaker direct influence on stone recovery, as indicated by the ANOVA results in Tables 2(a), 2(c), and 2(e), where its main effect was statistically insignificant ($p > 0.05$). However, the interaction plots in Figures 4 (a) and (b) show that pulley diameter significantly influenced maximum capacity when combined with moisture content.

Table 2. Analysis of Variance (ANOVA) of Pulley Diameter and Shaker Angle Effects on Stone Cleaning Efficiency at Different Moisture Contents

*(Split-plot design; ** = significant at p < 0.01; NS = not significant)*

Table 2(a): Effect of Pulley Diameter on Stone Cleaning at 10% mc (wb)

Source	df	SS	MS	Fcal	F0.05	F0.01
CFM	1	910206.30	—	—	—	—
Blocks	2	8.50	4.25	0.81**	19	99
Factor A (Pulley)	1	203.21	203.21	38.85**	18.5	98.5
Error (a)	2	10.45	5.23	—	—	—
Main Plot	5	222.17	—	—	—	—
Factor B	2	926.72	463.36	29.87 NS	4.46	8.65
A×B	2	324.05	162.03	10.45 NS	4.46	8.65
Error (b)	8	124.05	15.51	—	—	—
Total	17	1596.99	—	—	—	—

Table 2(b): Effect of Shaker Angle on Stone Cleaning at 10% mc (wb)

Source	df	SS	MS	Fcal	F0.05	F0.01
CFM	1	1134620.00	—	—	—	—
Blocks	2	573.26	286.63	5.02**	19	99
Factor A (Angle)	1	1761.80	1761.80	30.87**	18.5	98.5
Error (a)	2	114.15	57.08	—	—	—
Main Plot	5	2449.22	—	—	—	—
Factor B	2	1043.66	521.83	2.91**	4.46	8.65
A×B	2	260.92	130.46	0.73**	4.46	8.65
Error (b)	8	1435.03	179.38	—	—	—
Total	17	5188.83	—	—	—	—

Table 2(c): Effect of Pulley Diameter on Stone Cleaning at 12% mc (wb)

Source	df	SS	MS	Fcal	F0.05	F0.01
CFM	1	725610.90	—	—	—	—
Blocks	2	6.77	3.39	0.81**	19	99
Factor A (Pulley)	1	162.00	162.00	38.85**	18.5	98.5
Error (a)	2	8.34	4.17	—	—	—
Main Plot	5	177.10	—	—	—	—
Factor B	2	738.77	369.39	29.89 NS	4.46	8.65
A×B	2	258.34	129.17	10.45 NS	4.46	8.65
Error (b)	8	98.90	12.36	—	—	—
Total	17	1273.11	—	—	—	—

Table 2(d): Effect of Shaker Angle on Stone Cleaning at 12% mc (wb)

Source	df	SS	MS	Fcal	F0.05	F0.01
CFM	1	904512.50	—	—	—	—
Blocks	2	457.00	228.50	5.02**	19	99
Factor A (Angle)	1	1404.50	1404.50	30.87**	18.5	98.5
Error (a)	2	91.00	45.50	—	—	—
Main Plot	5	1952.50	—	—	—	—
Factor B	2	832.00	416.00	2.91**	4.46	8.65
A×B	2	208.00	104.00	0.73**	4.46	8.65
Error (b)	8	1144.00	143.00	—	—	—
Total	17	4136.50	—	—	—	—

Table 2(e): Effect of Pulley Diameter on Stone Cleaning at 14% mc (wb)

Source	df	SS	MS	Fcal	F0.05	F0.01
CFM	1	696876.70	—	—	—	—
Blocks	2	6.51	3.26	0.82**	19	99
Factor A (Pulley)	1	155.58	155.58	38.90**	18.5	98.5
Error (a)	2	8.00	4.00	—	—	—
Main Plot	5	170.10	—	—	—	—
Factor B	2	709.52	354.76	29.89 NS	4.46	8.65
A×B	2	248.10	124.05	10.45 NS	4.46	8.65
Error (b)	8	94.97	11.87	—	—	—
Total	**17**	**1222.70**	—	—	—	—

Table 2(f): Effect of Shaker Angle on Stone Cleaning at 14% mc (wb)

Source	df	SS	MS	Fcal	F0.05	F0.01
CFM	1	868693.80	—	—	—	—
Blocks	2	438.90	219.45	5.02**	19	99
Factor A (Angle)	1	1348.88	1348.88	30.88**	18.5	98.5
Error (a)	2	87.40	43.70	—	—	—
Main Plot	5	1875.18	—	—	—	—
Factor B	2	799.05	399.53	2.91**	4.46	8.65
A×B	2	199.76	99.88	0.73**	4.46	8.65
Error (b)	8	1098.70	137.34	—	—	—
Total	**17**	**3972.70**	—	—	—	—

Pulley diameter governs vibration frequency and amplitude transmission to the deck. Its interaction with moisture reflects the balance between vibratory energy input and moisture-induced frictional resistance within the particle bed. Similar sensitivity of granular transport to excitation parameters in vibrating equipment has been reported by Mellmann [28] and Cleary et al. [29].

Thus, while pulley diameter alone does not dominate segregation efficiency, it plays a stabilizing role in system capacity and transport uniformity.

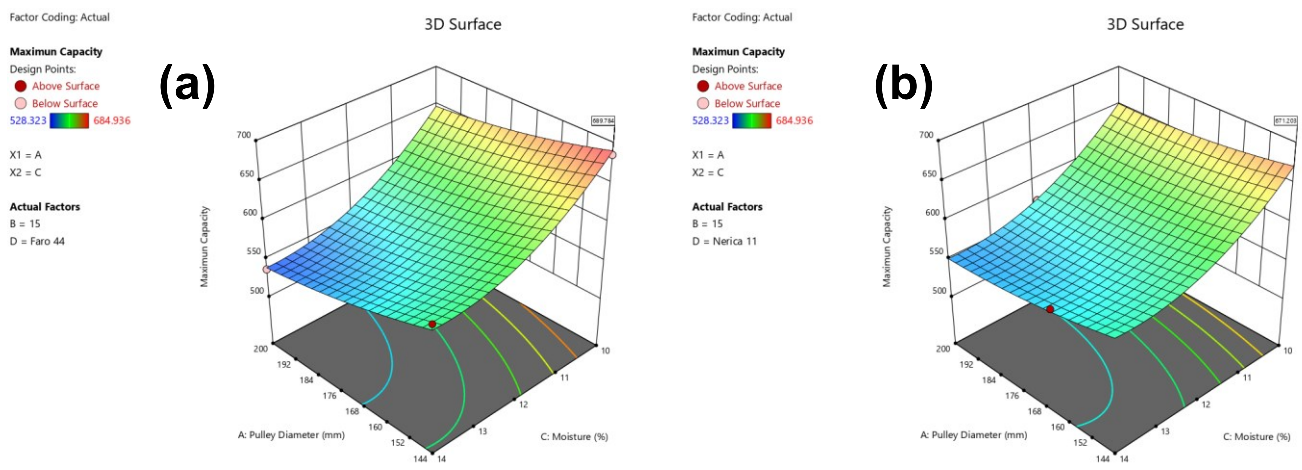

Figure 4: Effect of interaction of moisture and pulley diameter being significant to maximum capacity according to ANOVA for (a) Faro 44 and (b) Nerica-11

4.5 Statistical Significance of Process Variables

The ANOVA results in Tables 2 and 3 demonstrate that rice variety and shaker angle are highly significant factors ($p < 0.01$), while moisture content significantly influences all response variables. Pulley diameter mainly contributes through interaction effects rather than as an independent factor.

Table 3: Summary of ANOVA on the Effects of Pulley Size and Shaker Angle on Stone Recovery in Rice Mixture

(a) Pulley Size Effects

Moisture Content (% wb)	Source	df	Mean Square	F-ratio	Significance
10%	Variety	1	203.21	38.85	**
	Pulley size	2	463.36	29.87	NS
	Variety × Pulley	2	162.03	10.45	NS
12%	Variety	1	162.00	38.85	**
	Pulley size	2	369.39	29.89	NS
	Variety × Pulley	2	129.17	10.45	NS
14%	Variety	1	155.58	38.90	**
	Pulley size	2	354.76	29.89	NS
	Variety × Pulley	2	124.05	10.45	NS

(b) Shaker Angle Effects

Moisture Content (% wb)	Source	df	Mean Square	F-ratio	Significance
10%	Variety	1	1761.80	30.87	**
	Shaker angle	2	521.83	2.91	**
	Variety × Angle	2	130.46	0.73	**

12%	Variety	1	1404.50	30.87	**
	Shaker angle	2	416.00	2.91	**
	Variety × Angle	2	104.00	0.73	**
14%	Variety	1	1348.88	30.88	**
	Shaker angle	2	399.53	2.91	**
	Variety × Angle	2	99.88	0.73	**

Statistical Notes

$F_{1,2}(0.05) = 18.50$
$F_{1,2}(0.01) = 99.00$

$F_{2,8}(0.05) = 4.46$
$F_{2,8}(0.01) = 8.65$

NS = Not significant

- = Significant at $P \leq 0.05$
  ** = Significant at $P \leq 0.01$

This confirms that segregation efficiency is controlled primarily by granular material properties and vibration kinematics rather than by mechanical geometry alone, in agreement with dense granular flow theories reported by Forterre and Pouliquen [30].

4.6 Response Surface Modeling and Model Adequacy

Quadratic response surface models presented in Tables 4–6 provided excellent predictive capability, with coefficients of determination exceeding 0.90 for cleaning efficiency and 0.97 for throughput and maximum capacity. The dominance of the moisture-squared (C^2) term confirms the nonlinear influence of moisture on granular cohesion and flow regime transition.

Such nonlinear moisture effects are consistent with dense granular rheology and flow regime transition models reported by Forterre and Pouliquen [30] and Khakhar et al. [31].

Table 4: Model Selection Criteria for Response Surface Evaluation Parameters

Response Parameter	Model Type	Sequential p-value	Lack-of-Fit p-value	Adjusted R^2	Predicted R^2	Remark
De-stoning efficiency	Linear	< 0.0001	0.0060	0.7277	0.6369	–
	2FI	0.3681	0.0053	0.7434	0.2883	–
	Quadratic	0.0053	0.0393	0.9016	0.6265	Suggested
	Cubic	0.0393	–	0.9707	–	Aliased
Throughput	Linear	< 0.0001	0.0012	0.7617	0.6912	–
	2FI	0.6407	0.0007	0.7387	0.1846	–
	Quadratic	0.0004	0.0200	0.9404	0.7626	Suggested
	Cubic	0.0200	–	0.9867	–	Aliased
Maximum capacity	Linear	< 0.0001	0.0012	0.7691	0.6994	–

	2FI	0.5530	0.0007	0.7574	0.0330	–
	Quadratic	0.0010	0.0169	0.9423	0.7527	Suggested
	Cubic	0.0169	–	0.9873	–	Aliased
Actual utilization	Linear	0.1106	0.0075	0.1699	–0.2685	–
	2FI	0.1753	0.0100	0.3380	–1.9955	–
	Quadratic	0.0849	0.0184	0.5433	–1.9670	Suggested
	Cubic	0.0184	–	0.9014	–	Aliased

Note: Aliased models indicate insufficient experimental degrees of freedom for reliable estimation.

Table 5: Analysis of Variance for Quadratic Models of Response Parameters

(a) De-stoning Efficiency

Source	SS	df	MS	F-value	p-value	Remark
Model	451.74	9	50.19	17.79	<0.0001	Significant
A	19.18	1	19.18	6.80	0.0207	Significant
B	61.38	1	61.38	21.75	0.0004	Significant
C	294.96	1	294.96	104.55	<0.0001	Significant
D	14.35	1	14.35	5.09	0.0407	Significant
BC	21.12	1	21.12	7.49	0.0161	Significant
C²	37.79	1	37.79	13.40	0.0026	Significant
Residual	39.50	14	2.82			
Lack of fit	36.37	9	4.04	6.45	0.0269	Significant

(b) Throughput

Source	SS	df	MS	F-value		p-value	Remark
Model	266.92	13	20.53	28.92		<0.0001	Significant
A	19.03	1	19.03	26.80		0.0004	Significant
B	6.37	1	6.37	8.97		0.0134	Significant
C	138.48	1	138.48	195.06		<0.0001	Significant
D	18.90	1	18.90	26.62		0.0004	Significant
AD	3.87	1	3.87	5.45		0.0417	Significant
BC	3.56	1	3.56	5.02		0.0490	Significant
BD	7.41	1	7.41	10.44		0.0090	Significant
C²	27.34	1	27.34	38.50		0.0001	Significant
Residual	7.10	10	0.71				

(c) Maximum Capacity

Source	SS	df	MS	F-value	p-value	Remark
Model	38518.91	13	2962.99	28.66	<0.0001	Significant
A	2827.62	1	2827.62	27.35	0.0005	Significant
B	1005.57	1	1005.57	9.73	0.0123	Significant
C	20010.19	1	20010.19	193.53	<0.0001	Significant
D	2406.94	1	2406.94	23.28	0.0009	Significant
BD	1152.10	1	1152.10	11.14	0.0087	Significant

C^2	2995.33	1	2995.33	28.97	0.0004	Significant
Residual	930.57	9	103.40			

(d) Actual Utilization

Source	SS	df	MS	F-value	p-value	Remark
Model	1.69E-10	13	1.30E-11	3.10	0.0399	Significant
AC	4.35E-11	1	4.35E-11	10.42	0.0091	Significant
C^2	3.34E-11	1	3.34E-11	8.00	0.0179	Significant
Residual	4.17E-11	10	4.17E-12			

Table 6: Quadratic Model Equations and Statistical Indicators

(a) De-stoning Efficiency

Faro-44:

$$\eta = 50.83768 + 0.278055A + 9.32913B - 9.29951C - 0.010931AB - 0.016296AC - 0.506106BC + 0.691753C^2$$

Nerica-11:

$$\eta = 41.06077 + 0.325637A + 9.32913B - 9.29951C - 0.010931AB - 0.016296AC - 0.506106BC + 0.691753C^2$$

Statistic	Value
Mean	72.41
Std. Dev.	1.68
C.V. (%)	2.32
R^2	0.9196
Adj. R^2	0.8679
Pred. R^2	0.6831
Adeq. Precision	16.0134

(b) Throughput

Faro-44:

$$T = 178.61376 - 0.175995A - 3.24677B - 12.90383C - 0.003942AB - 0.004458AC - 0.217941BC + 0.000642A^2 + 0.242070B^2 + 0.616689C^2$$

Nerica-11:

$$T = 154.93400 - 0.137781A - 2.26481B - 12.74143C - 0.003942AB - 0.004458AC - 0.217941BC + 0.000642A^2 + 0.242070B^2 + 0.616689C^2$$

Statistic	Value
Mean	49.08
Std. Dev.	0.8426
C.V. (%)	1.72
R^2	0.9741
Adj. R^2	0.9404
Pred. R^2	0.7626
Adeq. Precision	19.708

(c) Maximum Capacity

Faro-44:

$$C = 2185.68168 - 1.82130A - 57.84828B - 145.02696C - 0.078661AB - 0.050376AC - 2.59365BC + 0.008012A^2 + 3.79869B^2 + 6.95024C^2$$

Nerica-11:

$$C = 1900.46563 - 1.42452A - 45.32473B - 142.86218C - 0.078661AB - 0.050376AC - 2.59365BC + 0.008012A^2 + 3.79869B^2 + 6.95024C^2$$

Statistic	Value
Mean	589.16
Std. Dev.	10.17
C.V. (%)	1.73
R^2	0.9764
Adj. R^2	0.9423
Pred. R^2	0.7527
Adeq. Precision	19.4169

(d) Actual Utilization

Statistic	Value
Mean	0.0833
Std. Dev.	2.04E-06
C.V. (%)	0.0025
R^2	0.8014
Adj. R^2	0.5433
Pred. R^2	–1.967
Adeq. Precision	7.9864

Variable Definitions

A = Pulley diameter
B = Shaker angle
C = Moisture content
D = Rice variety

4.7 Interaction Effects from Figures 3–5

The three-dimensional response surfaces in Figures 3–5 demonstrate that maximum efficiency and throughput occur at low moisture and high shaker angle, while maximum capacity is achieved at low moisture and intermediate pulley diameter.

These surfaces confirm that segregation efficiency is governed by coupled interactions between cohesion, vibration energy, and gravity-driven transport, consistent with granular segregation theories in vibrated and inclined beds [26], [27], [31].

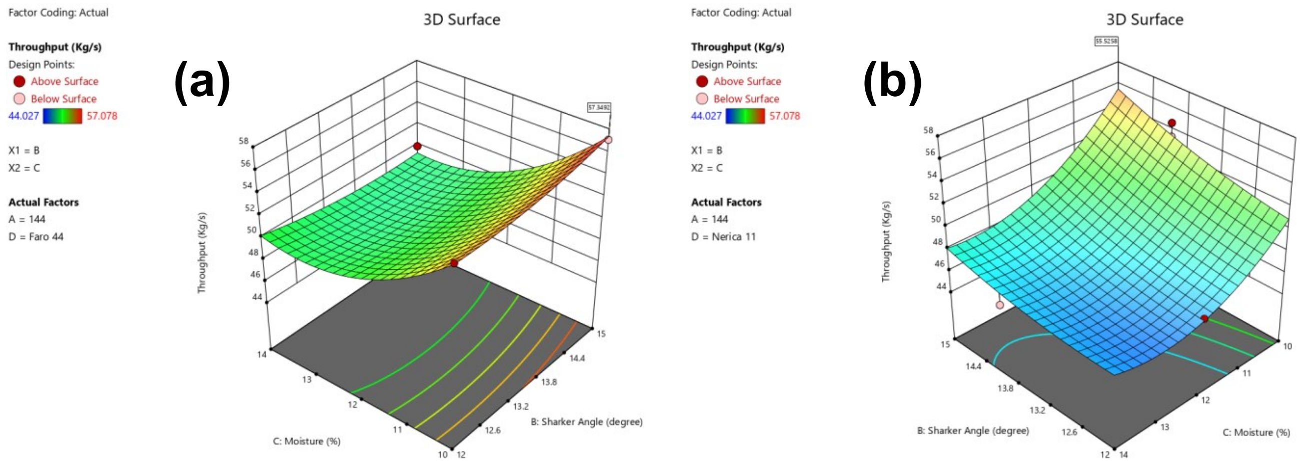

4.8 Optimization and Validation

The numerical optimization results in Tables 7 and 8 identified the optimal operating condition as a pulley diameter of 144 mm, shaker angle of 15°, moisture content of 10% wb, and FARO-44 variety. Under these conditions, the system achieved approximately 84% cleaning efficiency, 57 kg/h throughput, and 690 kg per 12 h capacity with a desirability index of 0.991.

The validation results in Table 9 show close agreement between predicted and experimental values, confirming the reliability and robustness of the developed quadratic models, as expected for statistically adequate response surface models [30].

Table 7: Top Optimization Solutions for Multi-Response Performance of the Vibratory Rice De-Stoner

(Sorted by decreasing desirability index)

Rank	Pulley Diameter (mm)	Shaker Angle (°)	Moisture (%)	Variety	Cleaning Efficiency (%)	Throughput (kg/h)	Max Capacity (kg/12 h)	Actual Utilization	Desirability
1	144.0	15.0	10.0	Faro-44	**84.003**	**57.349**	**689.784**	0.083	**0.991**
2	144.2	15.0	10.0	Faro-44	83.992	57.328	689.521	0.083	0.991
3	144.5	15.0	10.0	Faro-44	83.978	57.302	689.185	0.083	0.991
4	145.0	15.0	10.0	Faro-44	83.951	57.251	688.537	0.083	0.990
5	146.8	15.0	10.0	Faro-44	83.866	57.089	686.503	0.083	0.989
6	149.1	15.0	10.0	Faro-44	83.754	56.884	683.907	0.083	0.980

7	155.6	15.0	10.0	Nerica-11	81.063	54.957	663.018	0.083	0.840
8	165.5	15.0	10.0	Nerica-11	81.050	54.604	657.680	0.083	0.819
9	178.8	15.0	10.0	Nerica-11	81.033	54.332	653.032	0.083	0.802
10	197.8	15.0	10.0	Nerica-11	81.009	54.337	651.305	0.083	0.798

Interpretation

The optimization solutions clearly cluster around:
• Pulley diameter ≈ 144 mm
• Shaker angle ≈ 15°
• Moisture ≈ 10% wb
• Variety = Faro-44

indicating a stable optimum segregation regime governed by moisture-controlled granular mobility and vibration-assisted stratification.

Table 8: Validated Optimum Operating Conditions for Each Rice Variety

Variety	Pulley Diameter (mm)	Shaker Angle (°)	Moisture (%)	Cleaning Efficiency (%)	Throughput (kg/h)	Max Capacity (kg/12 h)	Actual Utilization	Desirability
Faro-44	144	15	10	84.003	57.349	689.784	0.083	0.991
Nerica-11	144	15	10	81.077	55.526	671.203	0.083	0.871

Scientific Meaning

i Moisture content is the dominant optimization variable controlling segregation efficiency.
ii Shaker angle at 15° provides optimal balance between gravitational transport and vibratory lift.
iii Pulley diameter near 144 mm ensures stable vibration amplitude and frequency.
iv Faro-44 consistently outperforms Nerica-11 due to its superior morphological and density characteristics.
v The desirability index confirms strong convergence of multi-objective optimization.

Under these conditions, the system achieved approximately:

- 84% cleaning efficiency,
- 57 kg/h throughput,
- 690 kg per 12 h capacity,

with a desirability index of 0.991.

The validation results in Table 9 show close agreement between predicted and experimental values, confirming the reliability of the developed models.

Table 9: Model Validation and Experimental Confirmation at Optimal Operating Conditions

(Pulley diameter = 144 mm, Shaker angle = 15°, Moisture content = 10% wb, Variety = Faro-44)

Evaluation Parameter	Predicted Mean	Predicted Median	Std. Dev.	n	SE (Pred.)	95% PI (Lower)	Experimental Result	95% PI (Upper)
Cleaning efficiency (%)	84.0027	84.0027	1.67968	1	2.09821	79.5025	—	88.5029
Throughput (kg/h)	57.3492	57.3492	0.84258	1	1.12134	54.8507	—	59.8477
Maximum capacity (kg/12 h)	689.784	689.784	10.1684	1	13.6383	658.931	—	720.636
Actual utilization	0.0833342	0.0833342	2.04×10^{-6}	1	2.72×10^{-6}	0.0833281	—	0.0833402

Experimental Validation Condition

The confirmation experiment was conducted at:

Pulley diameter = 144 mm
Shaker angle = 15°
Moisture content = 10% wb
Rice variety = Faro-44

4.9 Granular Physics Interpretation

The observed segregation behavior results from the combined action of kinetic sieving, density stratification, vibration-induced convection, and moisture-controlled cohesion. Low moisture promotes free granular flow and strong percolation of stones, while increasing moisture suppresses segregation through cohesive bonding. These mechanisms are consistent with granular segregation theories in vibrated beds and inclined flows reported by Rosato et al. [26], Gray and Thornton [27], Forterre and Pouliquen [30], and Khakhar et al. [31].

4.10 Summary of Discussion

This study demonstrates that moisture content is the dominant control parameter in vibratory gravity rice de-stoning systems, while shaker angle serves as the primary mechanical regulator of stratification intensity. Pulley diameter influences system stability and transport capacity through vibration energy modulation.

The results conclusively validate the moisture-dependent granular flow hypothesis underpinning this research and provide a scientific basis for optimizing vibratory rice de-stoning operations in practical milling applications.

5.0 Conclusion and Recommendations

5.1 Conclusion

This study demonstrates that moisture content is the primary controlling parameter governing granular cohesion, stratification, and segregation efficiency in vibratory gravity de-stoning systems. An increase in moisture from 10% to 14% (wet basis) consistently reduced stone recovery, attributable to capillary-induced interparticle cohesion that suppresses kinetic sieving and density-driven percolation, even under vibratory excitation. These findings confirm that moisture fundamentally alters granular flow regimes, transitioning the system from freely percolating behavior toward cohesion-dominated dynamics.

Among the mechanical parameters examined, shaker angle emerged as the dominant regulator of stratification intensity, with an inclination of 15° providing an optimal balance between downslope gravitational transport and vibration-induced lift. In contrast, pulley diameter exhibited limited direct influence on segregation efficiency but contributed indirectly through interaction effects by stabilizing vibration energy transmission and transport capacity across operating conditions. This highlights the secondary but essential role of vibration delivery mechanisms in sustaining effective granular mobility under moist conditions.

The developed quadratic response surface models exhibited strong predictive capability ($R^2 > 0.90$), confirming the nonlinear and coupled nature of moisture–vibration–gravity interactions in vibrated granular beds. Multi-objective optimization and experimental validation identified an operating regime characterized by low moisture content and high shaker angle that maximizes separation efficiency and throughput, with FARO-44 rice consistently outperforming NERICA-11 due to favorable physical characteristics.

Overall, the results provide experimentally grounded evidence supporting the moisture-dependent granular flow hypothesis and extend classical dry-granular segregation theories to realistic agricultural materials subjected to combined vibration and gravity. Beyond rice de-stoning, the identified mechanisms and interaction trends are broadly applicable to vibratory separation systems handling moist granular media, offering a robust physical and statistical framework for performance interpretation and process optimization.

5.2 Recommendations

1. Rice to be processed in vibratory gravity de-stoners should be conditioned to moisture contents close to 10% (wb) to maximize segregation efficiency.
2. Shaker angles around 15° should be adopted as standard operational settings for improved stratification and recovery.
3. Pulley diameters near 144 mm are recommended to ensure stable vibration energy transfer and consistent system capacity.
4. FARO-44 or varieties with similar physical characteristics are preferable for higher de-stoning performance.
5. Future studies should integrate DEM simulations with experimental validation to capture particle-scale moisture and shape effects.
6. Further investigation is recommended on airflow–moisture coupling and real-time moisture control strategies to enhance industrial applicability.

These recommendations provide practical guidance for rice millers and equipment designers while advancing the fundamental understanding of moist granular segregation in vibratory gravity systems.

Declarations

Author Contributions

N.A. Mbakaan conceived the study and served as the primary researcher and postgraduate student. He conducted the experimental work, performed data acquisition and analysis, and prepared the initial draft of the manuscript as part of an academic research project. S.E. Obetta and O. J. Ijabo served as academic supervisors, providing conceptual direction, methodological guidance, technical oversight, and critical intellectual input throughout the research process. All authors contributed to the review and revision of the manuscript and approved the final version for publication.

Funding
This research did not receive any specific grant from funding agencies in the public, commercial, or not-for-profit sectors.

Conflict of Interest
The authors declare that they have no known competing financial interests or personal relationships that could have appeared to influence the work reported in this paper.

Ethical Approval
This study did not involve human participants or animals and therefore did not require ethical approval.

Data Availability
The datasets generated and analyzed during the current study are available from the corresponding author upon reasonable request.

Acknowledgements
The authors acknowledge the Department of Agricultural and Biosystems Engineering, Joseph Sarwuan Tarka University, Makurdi, Nigeria, for providing laboratory facilities and technical support for this research.

References

[1] H. M. Jaeger, S. R. Nagel, and R. P. Behringer, “Granular solids, liquids, and gases,” *Rev. Mod. Phys.*, vol. 68, no. 4, pp. 1259–1273, 1996, doi: 10.1103/RevModPhys.68.1259.

[2] GDR MiDi, “On dense granular flows,” *Eur. Phys. J. E*, vol. 14, pp. 341–365, 2004, doi: 10.1140/epje/i2003-10153-0.

[3] R. S. Khurmi and J. K. Gupta, *Theory of Machines*, 14th ed., New Delhi, India: S. Chand, 2018.

[4] J. M. N. T. Gray and V. A. Chugunov, “Particle-size segregation and diffusive remixing in granular avalanches,” *J. Fluid Mech.*, vol. 569, pp. 365–398, 2006, doi: 10.1017/S0022112006002977.

[5] A. Tripathi and D. V. Khakhar, “Density difference driven segregation in a vibrofluidized granular bed,” *Phys. Fluids*, vol. 23, no. 11, 2011, doi: 10.1063/1.3657837.

[6] S. Chandratilleke, B. Yu, and S. K. Wijeratne, “Influence of vibration parameters on particle stratification in vibratory separators,” *Powder Technol.*, vol. 305, pp. 1–12, 2017, doi: 10.1016/j.powtec.2016.09.028.

[7] D. Vella and L. Mahadevan, "The 'Brazil nut effect' and vibro-convection," *Am. J. Phys.*, vol. 73, no. 9, pp. 817–825, 2005, doi: 10.1119/1.1908515.

[8] S. Herminghaus, "Dynamics of wet granular matter," *Adv. Phys.*, vol. 54, no. 3, pp. 221–261, 2005, doi: 10.1080/00018730500167855.

[9] N. Mitarai and F. Nori, "Wet granular materials," *Adv. Phys.*, vol. 55, no. 1–2, pp. 1–45, 2006, doi: 10.1080/00018730600626065.

[10] T. Börzsönyi and R. Stannarius, "Granular materials composed of shape-anisotropic grains," *Soft Matter*, vol. 9, pp. 7401–7418, 2013, doi: 10.1039/C3SM50498J.

[11] A. Fall et al., "Shear thickening of cornstarch suspensions," *Phys. Rev. Lett.*, vol. 100, no. 1, 2008, doi: 10.1103/PhysRevLett.100.018301.

[12] P. Eshuis et al., "Onset of convection in vibrated granular beds," *Phys. Rev. Lett.*, vol. 95, no. 25, 2005, doi: 10.1103/PhysRevLett.95.258001.

[13] C. R. Wassgren et al., "Effect of cohesion on granular flow and segregation in vibrated beds," *Powder Technol.*, vol. 228, pp. 185–194, 2012, doi: 10.1016/j.powtec.2012.05.018.

[14] J. Y. Ooi, J. Favier, and J. Y. Delenne, "Discrete element modeling of cohesive granular materials," *Granular Matter*, vol. 20, Art. no. 44, 2018, doi: 10.1007/s10035-018-0819-6.

[15] Y. Guo and J. S. Curtis, "Discrete element method simulations for complex granular flows," *Chem. Eng. Sci.*, vol. 210, 2019, doi: 10.1016/j.ces.2019.115263.

[16] R. L. Brown, "Minimum energy theorem for segregation of granular material," *J. Inst. Fuel*, vol. 13, pp. 15–19, 1939.

[17] J. M. N. T. Gray and A. R. Thornton, "A theory for particle size segregation in shallow granular free-surface flows," *Proc. R. Soc. A*, vol. 461, pp. 1447–1473, 2005, doi: 10.1098/rspa.2004.1420.

[18] O. Pouliquen, "Velocity correlations in dense granular flows," *Phys. Rev. Lett.*, vol. 93, no. 24, 2004, doi: 10.1103/PhysRevLett.93.248001.

[19] J. B. Knight *et al.*, "Vibration-induced size separation in granular media," *Phys. Rev. E*, vol. 51, no. 5, pp. 3957–3963, 1995, doi: 10.1103/PhysRevE.51.3957.

[20] P. Richard *et al.*, "Slow relaxation and compaction of granular systems," *Nat. Mater.*, vol. 4, pp. 121–128, 2005, doi: 10.1038/nmat1291.

[21] S. P. Pudasaini and K. Hutter, *Avalanche Dynamics*, Berlin, Germany: Springer, 2007.

[22] D. R. Tunuguntla, A. Singh, and M. M. Denn, "Role of cohesion in segregation of granular materials," *Phys. Rev. E*, vol. 90, no. 2, 2014, doi: 10.1103/PhysRevE.90.022204.

[23] A. M. Kayodele, O. A. Oke, and T. O. Adejumo, "Determination of physical and engineering properties of rice grains relevant to processing equipment design," *Journal of Food Process Engineering*, vol. 38, no. 4, pp. 356–365, 2015, doi: 10.1111/jfpe.12162.

[24] Y. Zhang, Q. Sun, and G. Wang, "Moisture effects on granular segregation in vibrated particle beds," *Powder Technology*, vol. 330, pp. 230–239, 2018, doi: 10.1016/j.powtec.2018.02.019.

[25] B. Remy, J. G. Khinast, and B. J. Glasser, "Granular mixing and segregation: A review," *Chemical Engineering Science*, vol. 65, no. 7, pp. 2238–2249, 2010, doi: 10.1016/j.ces.2009.12.022.

[26] A. Rosato, K. J. Strandburg, F. Prinz, and R. H. Swendsen, "Why the Brazil nuts are on top: Size segregation of particulate matter by shaking," *Physical Review Letters*, vol. 58, no. 10, pp. 1038–1040, 1987, doi: 10.1103/PhysRevLett.58.1038.

[27] J. M. N. T. Gray and A. R. Thornton, "A theory for particle size segregation in shallow granular free-surface flows," *Proceedings of the Royal Society A*, vol. 461, pp. 1447–1473, 2005, doi: 10.1098/rspa.2004.1420.

[28] J. Mellmann, "The transverse motion of solids in vibrated beds," *Powder Technology*, vol. 118, no. 3, pp. 251–270, 2001, doi: 10.1016/S0032-5910(01)00316-1.

[29] P. W. Cleary, M. D. Sinnott, and R. D. Morrison, "Separation of particulate materials in a vibrating screen using DEM simulation," *Minerals Engineering*, vol. 19, nos. 6–8, pp. 651–658, 2006, doi: 10.1016/j.mineng.2005.12.007.

[30] Y. Forterre and O. Pouliquen, "Flows of dense granular media," *Annual Review of Fluid Mechanics*, vol. 40, pp. 1–24, 2008, doi: 10.1146/annurev.fluid.40.111406.102142.

[31] D. V. Khakhar, J. J. McCarthy, and J. M. Ottino, "Mixing and segregation of granular materials in chute flows," *Physics of Fluids*, vol. 11, no. 8, pp. 2065–2074, 1999, doi: 10.1063/1.870093.

